

Insights into the galactic cosmic-ray source from the TIGER experiment

J.T. Link^{*,||}, L.M. Barbier^{*}, W.R. Binns[†], E.R. Christian^{*}, J.R. Cummings^{*},
S. Geier[‡], M.H. Israel[†], K. Lodders[‡], R.A. Mewaldt[‡],
J.W. Mitchell^{*}, G.A. de Nolfo^{*,**}, B.F. Rauch[‡], S.M. Schindler[‡],
L.M. Scott[†], R.E. Streitmatter[‡], E.C. Stone[‡], C.J. Waddington[§], and M.E. Wiedenbeck[¶]

^{*}NASA Goddard Space Flight Center, Greenbelt Maryland 20771

[†]Washington University in St. Louis, St. Louis Missouri 63130

[‡]California Institute of Technology, Pasadena, California 91125

[§]University of Minnesota, Minneapolis, Minnesota 55455

[¶]NASA Jet Propulsion Laboratory, Pasadena, California 91109

^{||}CRESST/USRA, Columbia Maryland 21044

^{**}CRESST/UMBC, Baltimore Maryland 21250

Abstract. We report results from 50 days of data accumulated in two Antarctic flights of the Trans-Iron Galactic Element Recorder (TIGER). With a detector system composed of scintillators, Cherenkov detectors, and scintillating optical fibers, TIGER has a geometrical acceptance of $1.7 \text{ m}^2\text{sr}$ and a charge resolution of 0.23 cu at Iron. TIGER has obtained abundance measurements of some of the rare galactic cosmic rays heavier than iron, including Zn, Ga, Ge, Se, and Sr, as well as the more abundant lighter elements (down to Si). The heavy elements have long been recognized as important probes of the nature of the galactic cosmic-ray source and accelerator. After accounting for fragmentation of cosmic-ray nuclei as they propagate through the Galaxy and the atmosphere above the detector system, the TIGER source abundances are consistent with a source that is a mixture of about 20% ejecta from massive stars and 80% interstellar medium with solar system composition. This result supports a model of cosmic-ray origin in OB associations previously inferred from ACE-CRIS data of more abundant lighter elements. These TIGER data also support a cosmic-ray acceleration model in which elements present in interstellar grains are accelerated preferentially compared with those found in interstellar gas.

Keywords: Cosmic Rays, Source, Fractionation

I. INTRODUCTION

Significant progress has recently been made in understanding the source of material for galactic cosmic rays (GCRs), as well the astrophysical location of their acceleration, and the role that atomic properties play in their acceleration process. Several experiments, most recently the ACE-CRIS experiment [1], have measured the GCR abundance ratio of $^{22}\text{Ne}/^{20}\text{Ne}$ and found that its source abundance is substantially higher than in the solar system. The most widely accepted explanation for this excess is the presence of ejecta from Wolf-Rayet

stars in the cosmic-ray source material [2],[3]. Based on the $^{22}\text{Ne}/^{20}\text{Ne}$ ratio measured on the ACE-CRIS experiment Higdon and Lingenfelter [4] have suggested a model in which the origin of cosmic ray source material and the site of acceleration is within OB associations, which are at the core of superbubbles. Type O and B stars are massive stars that reside almost entirely in OB associations and evolve into Wolf-Rayet stars. Higdon and Lingenfelter [4] and Binns et al. [1] have shown using independent approaches, that for elements lighter than Nickel, the cosmic ray source composition is consistent with a two-component model in which 20% of the source material comes from the outflow of massive stars and 80% comes from interstellar material of solar-system composition.

Understanding cosmic-ray source material composition also requires consideration of the atomic properties of the elements that may affect the acceleration process. It has been observed that some cosmic-ray elements have larger relative source abundances than in the solar system. This enhancement has been explained by a preferential acceleration of elements depending upon either their first ionization potential (FIP) [5] or condensation temperature [6],[7],[8]. Fractionation based on condensation temperature has received particular recent attention and has been explained by the preacceleration of atoms sputtered from dust grains in the interstellar medium causing an enhancement of refractory elements in the cosmic-rays.

In this paper we discuss results from the Trans-Iron Galactic Element Recorder (TIGER) instrument for elemental abundances between $26 \leq Z \leq 38$ from two high-altitude balloon flights over Antarctica. The first flight was in the 2001-02 Austral summer and lasted 32 days at an average altitude of 36 km (5.5 mb pressure). The second flight was in the 2003-04 Austral summer

and lasted 18 days with an average altitude of 39 km (4.1 mb pressure). These flights have resulted in the best GCR abundance measurements to date of ^{31}Ga , ^{32}Ge and ^{34}Se , as well as an upper limit to the abundance of ^{33}As , and a preliminary measurement of the ^{38}Sr abundance. In this paper we will show that data from these flights are consistent with a cosmic-ray source in which the material is a mixture of about 20% ejecta of massive stars (including Wolf-Rayet stars and core-collapse supernova) and 80% interstellar material with a solar system composition, thus supporting the OB association origin of GCRs. Additionally, we show that refractory elements are preferentially accelerated over volatile elements by about a factor of 3-4.

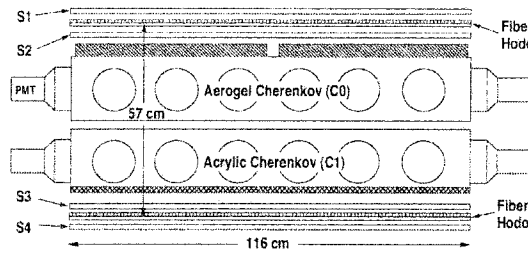


Fig. 1: TIGER Instrument cross section. S1, S2, S3 and S4 are the scintillation detectors, C0 the Aerogel Cherenkov and C1 the Acrylic Cherenkov. The fiber hodoscope consists of two orthogonally oriented planes of fibers placed between the top and bottom scintillator pairs.

II. INSTRUMENT DESCRIPTION AND DATA ANALYSIS

The TIGER instrument consists of a stack of scintillation detectors, Cherenkov detectors and a scintillating fiber hodoscope arranged as shown in Figure 1. This configuration gives the instrument a geometrical acceptance of $1.7 \text{ m}^2\text{sr}$. The scintillation detectors consist of St Gobain BC-416 plastic scintillator with dimensions $116 \times 116 \times 0.8 \text{ cm}$. Four wavelength shifter bars (St. Gobain BC-482) are placed around the perimeter of each scintillator with a small air gap separating the waveshifter bar from the scintillator. Each bar is 89 cm long with a $1.27 \times 1.27 \text{ cm}$ cross section and uses two Hamamatsu R1924 photomultiplier tubes (PMTs), with one coupled to each end of the bar to read out photons from the radiator.

The two Cherenkov detectors consist of a light collection box with dimensions $116 \times 116 \times 21 \text{ cm}$, each with 24 Burle S83006F PMTs collecting light from the four sides of the box (6 PMTs per side). The Cherenkov lightboxes have different radiators: the aerogel detector has a mosaic of four 3-cm thick pieces of silica aerogel with active area $51 \times 51 \text{ cm}$ and index of refraction 1.04. The acrylic detector has 114-cm square 1.06 cm thick acrylic radiator with index of

refraction 1.5.

The two hodoscope planes each consist of two layers of 1mm square scintillating fibers oriented perpendicular to each other. The individual fibers are formatted into tabs of 6 or 7 fibers and then these tabs are bundled in groups of 14 and formatted onto a Hamamatsu R1924 PMT. The fibers at one end are formatted so that fourteen adjacent tabs are bundled together, while at the other end, each of the adjacent fourteen tabs are formatted to a different PMT. This coding process is then repeated for the next set of fourteen adjacent tabs and allows us to uniquely identify which tab was hit using only 28 PMTs per fiber layer [9]. The calculated root-mean square position resolution of the hodoscope is 0.17 cm.

The charges of incident cosmic-ray nuclei that pass through the detector are determined by the signals from the upper two scintillation detectors (S1 and S2) and the two Cherenkov counters (C0 and C1). These summed PMT signals are corrected for gain differences, area nonuniformities and temporal variations. The fiber hodoscope provides the particle trajectory and allows for area nonuniformity corrections and a pathlength correction to the signal. The charge of particles with energies between 0.35 and 2.5 GeV/nucleon are determined by using the top two scintillation counters and the acrylic Cherenkov radiator. Particles with energies above 2.5 GeV/nucleon experience a relativistic rise which, if we used scintillators to measure their Z , would diminish our charge resolution. Instead, above 2.5 GeV/nucleon we use the acrylic and aerogel Cherenkov counters to achieve excellent charge resolution of these higher energy particles. Particles with energies less than 0.35 GeV/nucleon are below the threshold energy of the acrylic Cherenkov and cannot be analyzed by the instrument. We remove particles that interact in the instrument by requiring agreement of roughly one charge unit agreement between each detector used to determine the charge of the particle.

A charge histogram of the combined 2001 and 2003 TIGER dataset is shown in Figure 2. The charge resolution of the instrument is 0.23 cu. The smooth curve through the data is a multi-Gaussian maximum-likelihood fit which we use to derive relative abundances for most of our analysis. ^{27}Co and ^{29}Cu abundances are determined by a more refined analysis discussed further by Rauch *et al.* [10]. From the plots, one can see well-defined element peaks at ^{31}Ga , ^{32}Ge and ^{34}Se . At higher charges, the data are statistics limited although there is an indication of a peak at ^{38}Sr .

III. TIGER RESULTS AND THE GCR SOURCE

We have propagated our measurements to the top of the atmosphere, correcting for interactions in the

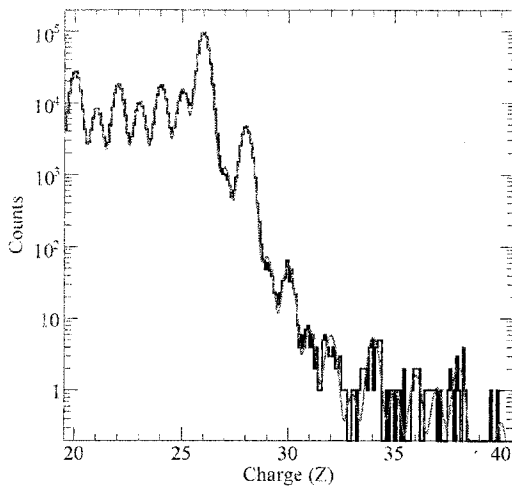


Fig. 2: Combined charge data from the 2001 and 2003 TIGER flights. The line shows a multiple-gaussian maximum likelihood fit to the data.

instrument and the atmosphere, as well as energy loss in the atmosphere [10], [11]. These “top-of-the-atmosphere abundances” relative to iron are plotted in Figure 3 along with the abundances of Zn, Ga and Ge measured by the HEAO-C2 instrument [12]. The TIGER results are consistent with those of HEAO-C2 but have smaller uncertainties due to better statistics. Also shown in Figure 3 (solid line) are the elemental abundances in the solar system for comparison with the measured abundances [13]. Both ^{30}Zn and ^{32}Ge are low relative to ^{26}Fe which is in agreement with an depletion of volatile elements in the acceleration process. The enhancement of ^{31}Ga is quite surprising. Our measured ^{31}Ga abundance is about equal to that of ^{32}Ge , whereas in the solar system the ratio of these elements is about 0.3. A possible explanation for this comes from Woosley and Heger [14] who have calculated the combined outflow from massive stars with initial mass ranging from 12 to 120 solar masses, after weighting by a Salpeter initial mass function (IMF). This represents the mass ejecta from OB associations where most type O and B stars reside. They find that the element most enhanced over solar-system abundances in this environment is ^{31}Ga , which has an enhancement factor over gallium in the solar system of approximately a factor of 30. This may account for the enhancement observed in the $^{31}\text{Ga}/^{32}\text{Ge}$ ratio.

To further investigate these results we derive elemental abundances at the GCRS using data from the HEAO-3 C2 experiment [15] for $Z < 26$ and TIGER data for $Z \geq 26$. Source propagation is done using a leaky-box propagation model [16] and a spherically symmetric modulation model [17] with modulation level $\phi = 850$ MV to allow comparison with the observations

made near earth. An assumed cosmic-ray source abundance is used and adjusted so that after applying the propagation model there is agreement with the top-of-the-atmosphere abundances. Figure 4 is a plot of the ratio of the derived galactic cosmic-ray source (GCRS) abundances to solar system (SS) abundances as a function of the elemental atomic mass. Refractory elements (with equilibrium condensation temperature greater than 1200K) are shown as closed circles and volatile elements (with condensation temperature less than 1200K) are shown as open circles [13]. The ratio of GCRS/SS is generally higher for refractory elements than volatile elements, but there is significant scatter, particularly for heavy elements, suggesting that the solar system abundances are not really the right source abundance to compare to.

As discussed earlier, there is evidence from the ACE-CRIS experiment that the cosmic-ray source composition is a 20%/80% mixture of material. If this is the case we should not be comparing our source abundances relative to solar system abundances but rather to the 20%/80% mixture. Figure 5 is a modification of Figure 4 with this changed ratio and there is a striking improvement in the organization of the data. The lines shown in Figure 5 are fits to the refractory and volatile data and show a clear mass dependence for both the refractory and volatile elements. The refractory elements have a mass (A) dependence of approximately $A^{2/3}$ and the volatile elements have a mass dependence of approximately A^1 . The oxygen datum in Figure 5 is consistent with a model of refractory fractionation despite where it appears on the figure because a significant fraction of oxygen can be found in dust grains [8], [18]. The amount expected to be sequestered in grains and hence enhanced in our abundances measurement is consistent with the experimental measurements [10].

We have found that there is good organization of our

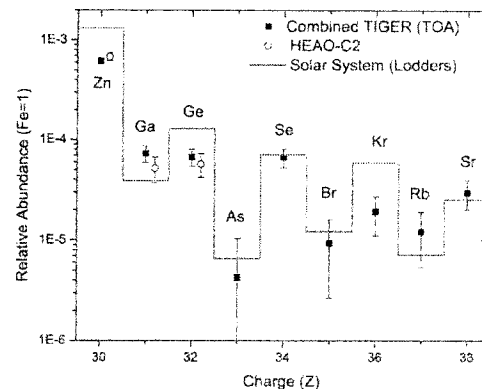


Fig. 3: TIGER and HEAO-C2 results relative to Fe compared with solar system abundances.

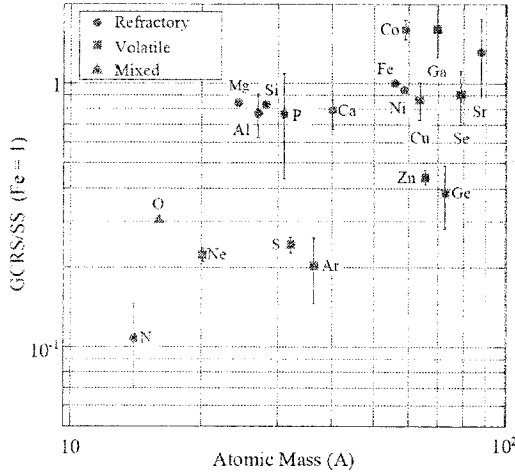


Fig. 4: Ratio of GCRS abundances to SS abundances vs. atomic mass (A). Refractory and volatile elements are designated by icon shape and color.

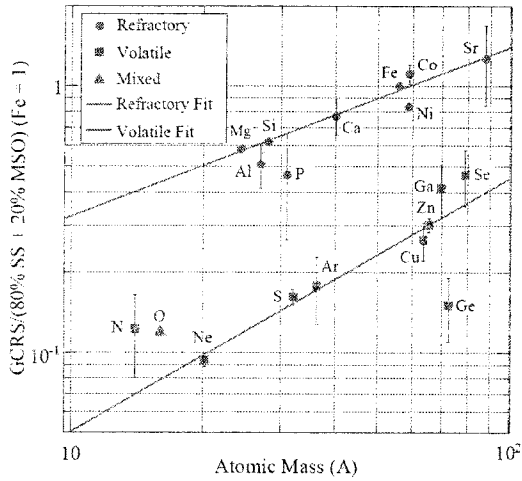


Fig. 5: Ratio of GCRS abundances to a mixture of 80% solar system and 20% massive star outflow versus atomic mass (A). Refractory and volatile elements are designated by icon shape and color. The lines are best fits to the volatile and refractory elements.

data where the percentage of material from the outflow of massive stars is between 15 and 25%. Therefore the precise value of this mixture is not tightly constrained. We have also looked at our results plotted versus first ionization potential to examine the possibility of preferential acceleration based on FIP. This was done for both the case of GCRS abundances versus a pure SS abundance and versus an 20%/80% mixture. We found significant scatter and disorder in both cases suggesting such an ordering is not correct [10].

The dramatic improvement in the ordering of the

volatile and refractory element abundances that occurs when compared to the 20%/80% mix provides strong evidence that galactic cosmic rays originate in OB associations. Additionally these abundances confirm the preferential acceleration of refractory elements compared to volatile elements and indicates that there is a mass dependence for both classes of elements. To better understand the origin and acceleration of cosmic rays, further high statistics measurements of ultra-heavy cosmic-ray elements are needed. Super-TIGER, a balloon instrument with almost an order of magnitude more collecting power than TIGER, is currently being developed for a first Antarctic launch in 2012. Super-TIGER will be able to measure elemental cosmic-ray abundances up to $Z=42$, with exploratory measurements up to $Z=60$ [19].

IV. ACKNOWLEDGEMENTS

We acknowledge the excellent contribution of the staff of the Columbia Scientific Balloon Facility, NASA Balloon Program Office and NSF Office of Polar Programs who supported and made possible the two Antarctic Balloon Flights. This research was supported by NASA Grants NNG05WCO4G and NNG05WC21G. The participation of K.L. was supported by NSF Grant AST0807356.

REFERENCES

- [1] Binns, W. R., et al. 2005, *ApJ*, 634, 351
- [2] Casse, M. & Paul, J. A. 1982, *ApJ*, 258, 860
- [3] Prantzos, N., et al. 1987, *ApJ*, 315, 209
- [4] Higdon, J. C. & Lingenfelter, R. E. 2003, *ApJ*, 590, 822
- [5] Casse, M. & Goret, P. 1978, *ApJ*, 221, 703
- [6] Epstein, R. I. 1980, *MNRAS*, 193, 723
- [7] Cesarsky, C. J. & Bibring, J. P. 1981, in *IAU Symp. 94, Origin of Cosmic Rays*, ed. G. Setti, G. Spada & A.W. Wolfendale (Dordrecht: Kluwer), 361
- [8] Meyer, J.-P., et al. 1997, *ApJ*, 487, 182
- [9] Lawrence, D. J., et al. 1999, *Nucl. Instr. & Meth. Phys. Res. A*, 420, 402
- [10] Rauch, B. F. et al. 2009, *ApJ*, 697, 2083
- [11] Rauch, B. F. 2008, PhD dissertation, Washington University, St. Louis
- [12] Byrnak, B., et al. 1983, *Proc. 18th Int. Cosmic Ray Conf. (Bangalore)*, 2, 29
- [13] Lodders, K. 2003, *ApJ*, 591, 1220
- [14] Woosley, S. E. & Heger, A. 2007, *Physics Reports*, 442, 269
- [15] Engelmann, J. J., et al. 1990, *Astronomy and Astrophysics* 233, 96
- [16] Wiedenbeck, M. E., et al. 2007, *Space Sci. Rev.*, 130, 415
- [17] Fisk, L. A. 1971, *J. Geophys. Res.*, 76, 221
- [18] Lingenfelter, R. E., et al. 1998, *ApJ*, 500, L153
- [19] De Nolfo, G.A. et al. 2009, *Proc 31st Int. Cosmic Ray Conf. (Lodz)*